Temperature-Induced Conformational Switch in Intestinal Fatty Acid Binding Protein (IFABP) Revealing an Alternative Mode for Ligand Binding†

Cecilia N. Arighi, Juan Pablo F. C. Rossi, and José M. Delfino*

Department of Biological Chemistry and Institute of Biochemistry and Biophysics (IQUIFIB), School of Pharmacy and Biochemistry, University of Buenos Aires, Junín 956, 1113 Buenos Aires, Argentina

Received November 27, 2002; Revised Manuscript Received March 19, 2003

ABSTRACT: IFABP is a small β-barrel protein with a short helix−turn−helix motif near the N-terminus that is thought to participate in the regulation of the uptake and delivery of fatty acids. In a previous work, we detected by near UV circular dichroism a reversible conformational transition of this protein occurring between 35 and 50 °C in the absence of fatty acids. The addition of the natural ligand oleic acid prevents this phenomenon. In both cases, the overall structure of the β-barrel is maintained. This thermal transition is also detected by the fluorescent probe bis-anilino naphthalene sulfonic acid (bisANS) but not by its monomer ANS. In the present work, we studied in detail the interaction of each compound with IFABP as a function of temperature and in the absence or in the presence of oleic acid. A contrasting behavior was observed for these probes: (i) IFABP is able to bind two molecules of bisANS but only one molecule of ANS and (ii) oleic acid can fully displace ANS but only partially bisANS. Three independent lines of evidence, namely, fluorescence spectroscopy, circular dichroism, and limited proteolysis, indicate that there is an equilibrium among different conformations of IFABP, which differ in the extent of flexibility of the helical domain. This equilibrium can be shifted by raising temperature. bisANS is able to probe a population of IFABP in an altered state, which is more susceptible to cleavage by clostripain as compared to the apo-form, whereas the conformation of IFABP bound to oleic acid is characteristically more ordered. These results highlight the idea of an enhanced flexibility exhibited by IFABP that bears importance on its transport function, supporting the role of a dynamic entry portal region for the fatty acid ligand.

Intracellular lipid binding proteins (iLBPs) constitute a family of low molecular weight proteins (12−15 kDa) with the putative general function of lipid trafficking (*1*). Members of this family include retinol binding proteins (CRBPs) (*2*), retinoic acid binding proteins (CRABPs) (*3*), sterol carrier proteins (*4*), and cytosolic fatty acid binding proteins (FABPs)[1] (*5*). FABPs share a similar three-dimensional structure that resembles a clamshell and consists of 10 antiparallel β-strands arranged as two nearly orthogonal β-sheets with five strands each, enclosing a cavity, which is the ligand binding site. This structure differs from most known globular proteins since its interior is occupied by a large solvent-filled cavity and a displaced hydrophobic core. The first two β-strands are separated by a helix−turn−helix motif (*5*). Helix II from this motif is thought to play an important regulatory role in the entry and exit of the ligand. This helix belongs to the so-called entry portal, a region that comprises also the two adjacent β turns (C−D and E−F) (*6*−*8*). The binding of the ligand is accompanied by some structural changes in this domain. For many members of iLBPs, an equilibrium has been proposed between at least two conformations (*6*−*10*), namely, an open (more flexible) state and a closed (more compact) state. In the case of IFABP, the latter would be stabilized by interactions between the protein and the fatty acid chain, as evidenced by comparison of the NMR structures of the apo- and holo-forms (*6*−*8*). In addition, a molecular dynamics simulation of apo-IFABP revealed that there are global conformational changes, which result in the transient exposure of the cavity to the bulk solvent (*11*).

In a recent work (*12*), we described a reversible conformational change that apo-IFABP undergoes between 30 and 50 °C, occurring well below the denaturation temperature of this protein (∼75 °C). Aromatic residues as well as the extrinsic fluorescent probes ANS and its dimer bisANS (Scheme 1) were used as spectroscopic probes to monitor this transition. Differences were found between the apo- and holo-forms and also between the complexes with each bound fluorescent ligand as a function of temperature. This transition is prevented by the binding of the fatty acid ligand as revealed by near UV CD spectroscopy. On the other hand,

† This work was supported in part by grants from the National Research Council of Argentina (CONICET and SECYT), the University of Buenos Aires (UBACYT), Fundación Antorchas, and the European Union.

* To whom correspondence should be addressed. E-mail: delfino@qb.ffyb.uba.ar.

[1] Abbreviations: ANS, 1-anilino naphthalene-8-sulfonic acid; bisANS, 4,4′-dianilino-1,1′-binaphthyl-5,5′-disulfonic acid; CD, circular dichroism; CRBP, cellular retinol binding protein; FRET, fluorescence resonance energy transfer; HFABP, heart fatty acid binding protein; IFABP, intestinal fatty acid binding protein. Holo-IFABP denotes the protein occupied with the fatty acid ligand; apo-IFABP is the protein devoid of ligands; NMR, nuclear magnetic resonance; $[\theta]_M$, molar ellipticity; SDS−PAGE, sodium dodecyl sulfate−polyacrylamide gel electrophoresis.

10.1021/bi020680d CCC: $25.00
Published on Web 05/24/2003

Scheme 1

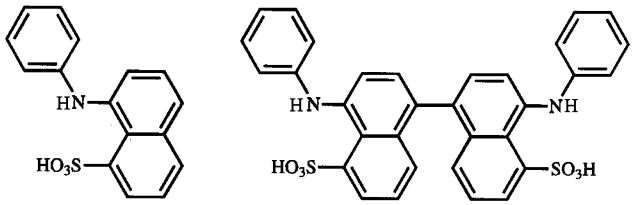

ANS bisANS

far UV CD and tryptophan fluorescence spectroscopies suggest that the β-barrel structure is not involved in the changes observed. An enhanced flexibility occurring at the helical domain was put forward to interpret these data. In addition, bisANS, but not ANS, was able to probe this transition. Although they share similar spectroscopic properties, the different size of these fluorescent probes might enable each one to sense a different protein environment.

In this paper, we present a comprehensive binding study of IFABP employing different methodologies, such as fluorescence and CD spectroscopies, together with results from partial proteolysis in the absence or in the presence of ligands. This allowed us to extend the current view on structural as well as thermodynamic aspects of this protein, in particular, regarding the involvement of the thermal transition in the ligand binding activity.

MATERIALS AND METHODS

Materials. Rat IFABP cDNA in the plasmid pET11a was expressed in the *Escherichia coli* strain BL21(DE3), and the protein was purified as described previously (*12*). All chemicals for bacteria growth media were purchased from Merck (Darmstadt, Germany); buffers, L-tryptophan, and quinine hydrochloride were purchased from Sigma-Aldrich (St. Louis, MO); ANS and bisANS were supplied by Molecular Probes Inc. (Eugene, OR); and sequencing grade clostripain (endoproteinase Arg-C) was purchased from PROMEGA (Madison, WI).

Ligands. In experiments involving holo-IFABP, a fresh solution of oleic acid in 20 mM potassium phosphate buffer, pH 7.4 (buffer A) was prepared from a stock solution in ethanol (4 mM), sonicated for 5 min, and added under stirring to IFABP dissolved in the same buffer at a 4:1 molar ratio. The variation of pH with temperature was less than 0.02 units in the range of 25−40 °C. The final concentration of ethanol in the assay never exceeded 2%.

The purity of ANS and bisANS was checked by TLC developed in chloroform/methanol/acetic acid (14:5:1, by vol.). Spots on the TLC plates were detected by their intrinsic fluorescence and by quenching under illumination with a UV source (254 nm) and/or staining with iodine vapor. Analysis of each probe showed a single spot with an R_F of approximately 0.50 or 0.20, for ANS or bisANS, respectively, values that agree with those obtained by Daniel and Weber (*13*). Solutions of ANS or bisANS were prepared in buffer A from 5 mM stock solutions in ethanol and were kept in the dark at 4 °C. The final concentration of each probe was determined spectrophotometrically using extinction coefficients in water ($cm^{-1}\ M^{-1}$) of 4950 (350 nm) for ANS and 17 000 (385 nm) for bisANS (*13*). In all cases, the buffers employed were vacuum degassed.

Fluorescence Measurements. Steady state fluorescence measurements were performed in an Aminco Bowman Series 2 spectrofluorometer operating in the ratio mode and equipped with a thermostated holder connected to a circulating water bath. A 1 cm path cuvette sealed with a Teflon cap was used. Alternatively, a 0.3 cm path cuvette was used to reduce the inner filter effect when needed. Temperature was measured directly with an electronic thermocouple immersed in the sample. For both fluorescent probes, excitation wavelength was 400 nm, and emission was collected in the range of 420−600 nm. Spectral slit-widths were set to 4 and 8 nm for the excitation and emission monochromators, respectively. Data were corrected for dilution and inner filter effects as indicated (*14*); and for each spectrum, the wavelength of the center of mass $\langle\lambda_p\rangle$ (in nm) was calculated (*15*). To minimize light scattering, samples were filtered through a 0.22 μm Millipore Millex-GV membrane previous to each experiment.

Titration Experiments. The binding of ANS or bisANS to IFABP was monitored by changes in the fluorescence intensity of the dyes, shifts of the center of mass of the spectra corresponding to the bound dyes, or by measuring the efficiency of energy transfer (EFRET). In all cases, protein concentration ranged from 0.5 to 2 μM. The measurements were recorded at 28 and 39 °C, after equilibration for 2 min.

Reverse Titration (at a Fixed Ligand Concentration). To estimate the enhancement in fluorescence intensity at saturation (ΔF_{max}), the experiment was run as follows. IFABP was repeatedly added to a ligand solution (1 μM) equilibrated at the corresponding temperature. A double reciprocal plot of the total concentration of protein ($[P]_{total}$) as a function of the enhancement in fluorescence intensity observed (ΔF) allowed us to calculate the extrapolated value at infinite protein concentration ($1/[P]_{total} \rightarrow 0$). This value represents the maximum fluorescence intensity attainable by the ligand when it is completely bound to the protein. ΔF is the difference between the observed fluorescence intensity in the presence (F) and in the absence (F_o) of IFABP.

Titration at a Constant Protein Concentration. This experiment was performed to obtain the best estimates for the binding parameters K_d and n, the dissociation constant, and the number of binding sites, respectively. In this case, the ligand was repeatedly added to a solution containing IFABP in buffer A or to buffer A (blank). Data were fitted by nonlinear regression to either a model of n identical, noninteracting binding sites (eq 1) or to a model of two nonidentical, noninteracting binding sites (eq 3) (*16*) using Sigma Plot software (SPSS Inc., version 5.0). In both cases, we considered $[L]_{free} \approx [L]_{total}$:

$$\Delta F = \frac{n[L]_{total}\Delta F_{max}}{(K_d + [L]_{total})} \quad (1)$$

$$\frac{b}{[L]_{total}} = \frac{n}{K_d} - \frac{b}{K_d} \quad (2)$$

where eq 2 is the Scatchard representation (*17*) of eq 1, and b, the ligand bound to the protein, equals $\Delta F/\Delta F_{max}$.

$$\Delta F = \frac{([L]_{total}\Delta F_{P1L}/K_{d1} + 2[L]^2_{total}\Delta F_{max}/K_{d1}K_{d2})}{\left(1 + \frac{[L]_{total}}{K_{d1}} + \frac{[L]^2_{total}}{K_{d1}K_{d2}}\right)} \quad (3)$$

where ΔF_{P1L} is the molar fluorescence change upon ligand binding to the first site, ΔF_{max} is determined independently by performing a reverse titration as previously explained, and K_{d1} and K_{d2} are the corresponding dissociation constants of the ligand to each site.

Calculation of Quantum Yield. The quantum yields (ϕ, eq 4) of IFABP or of the fluorescent ligands bound to this protein were obtained with reference to a compound of known quantum yield (ϕ_{ref}) (*18*). For IFABP, we used as standard, a solution of L-tryptophan in water at 25 °C (ϕ = 0.14, range of 300−450 nm), and for ANS/bisANS we employed a solution of quinine in 1 N H_2SO_4 (ϕ = 0.55, range of 400−600 nm) at 25 °C.

$$\phi = \frac{\phi_{ref} I A_{ref}}{I_{ref} A} \quad (4)$$

where I is the total corrected fluorescence intensity of the sample, and A is its absorbance at the excitation wavelength; the subindex corresponds to the parameters of the reference sample.

Competition Experiments. Displacement of bound ANS or bisANS to IFABP by oleic acid was measured by the decrease of fluorescence intensity with increasing oleic acid concentration. The apparent dissociation constant (K_{dapp}) was calculated by fitting the data to

$$\Delta F = \frac{\Delta F_o}{\left[1 + \frac{[\text{oleic acid}]}{K_{dapp}}\right]} + \Delta F_{res} \quad (5)$$

where ΔF represents the difference between the observed fluorescence intensity in the presence of protein subtracted from the contribution of the probe at the same concentration of oleic acid; ΔF_o is the contribution to the fluorescence intensity in the absence of oleic acid; and ΔF_{res} is a term that accounts for the remnant fluorescence at very large oleic acid concentration. These experiments were performed at three different concentrations of probe (5, 10, and 15 μM) and as a function of temperature.

To evaluate whether possible photocrosslinking between bisANS and IFABP had occurred as a consequence of irradiation during fluorescence measurements, the fluorescence intensity of a solution containing 2 μM IFABP and 15 μM bisANS was recorded before splitting it into three samples that were treated as follows. A first sample was kept in the dark for 30 min at 20 °C, the second sample was placed in the fluorometer and its fluorescence signal was measured as usual at intervals of 2 min for 30 min, and the third sample was irradiated with a 366 nm UV source for 10 min. After these treatments, the samples were dialyzed against buffer A, and the fluorescence intensity was measured again using the same settings of photomultiplier voltage, slit-width, and excitation and emission wavelengths, so that the observed values could be compared.

Resonance Energy Transfer Measurements. Samples of IFABP bound to ANS or bisANS were excited at 290 nm, and their spectra were recorded in the range of 310−550 nm. Excitation and emission slit-widths of 4 nm were used. Protein concentration was kept constant at 2 μM, and bisANS or ANS concentration was varied. The direct excitation of the acceptor (i.e., each fluorescent probe at each concentration assayed) was subtracted, and data were corrected by dilution and by absorption effects (*14*). The efficiency of FRET (EFRET) was calculated by comparing the fluorescence intensity of the donor in the absence (I_d) and in the presence of the acceptor molecule (I_{da}) (*14*):

$$EFRET = 1 - \frac{I_{da}}{I_d} \quad (6)$$

When necessary, a correction for fractional saturation was made as follows:

$$f_{sat} = \frac{[PL]}{[P]_{total}} \quad \text{and} \quad EFRET_{corr} = \frac{EFRET_{obs}}{f_{sat}} \quad (7)$$

where [PL] represents the concentration of protein bound to the fluorescent ligand estimated by using the values of K_d derived from titration experiments (*19*).

EFRET can be used to estimate the distance r (in Å) between chromophores by

$$r = R_o \sqrt[6]{\frac{1}{EFRET} - 1} \quad (8)$$

and

$$R_o = 9790\sqrt[6]{J\kappa^2 n^{-4}\phi_d} \quad (9)$$

where n is the refractive index of the medium (n = 1.4 for protein solutions), and κ^2 is the orientation factor (for this calculation a value of 2/3 was used, which assumes that the donor emission and acceptor absorption dipoles are randomly oriented). In addition to these parameters, for the estimation of R_o (in Å), which is the distance at which the energy transfer efficiency is 0.5, it is necessary to measure (i) the quantum yields (ϕ_d) of IFABP at 28 and at 39 °C and (ii) J, the spectral overlap integral between the donor emission spectrum ($F_d(\lambda_i)$) and the absorption spectrum of the acceptor ($\epsilon_a(\lambda_i)$).

$J = \sum_i F_d(\lambda_i)\epsilon_a(\lambda_i)\lambda_i^4$, in M^{-1} cm^3, where $F_d(\lambda_i) = F_i/\sum_j F_d(\lambda_j)$ is the fluorescence intensity of the donor relative to the integrated fluorescent measured over the whole spectrum, and $\epsilon_a(\lambda_i)$ is the molar extinction coefficient of the acceptor at each wavelength.

In the case of the pair IFABP−ANS, the values found for R_o (24.1 and 23.2 Å, at 28 and 39 °C, respectively) are close to that cited in the literature for the tryptophan−ANS pair (23 Å, ref *18*). This calculation assumes that FRET occurs from a single donor to a single acceptor. For IFABP, this is a good approximation because although two tryptophan residues are present in this molecule, only one of them (W82) contributes significantly to the fluorescence emission (*20*, *21*). In this regard, a tryptophan mutant of this protein (W6Y) showed a similar value of R_o (27 Å, ref *22*). However, when r was estimated using these values of R_o, the distances obtained (26.5 and 25.0 Å, at 28 and at 39 °C, respectively) were much larger than expected, given that there is inde-

pendent evidence that the donor−acceptor distance must be significantly shorter than the values shown above (5−7 Å, refs *12* and *22*). This emphasizes the need to obtain a realistic estimate of the orientation factor (κ^2) to obtain reliable values of distance.

In competition experiments monitored by FRET, the fluorescence intensity data of the bands appearing in the range of 410−550 nm were fitted to eq 5. Here, ΔF refers to the integrated fluorescence intensity observed in that wavelength range, whereas ΔF_o estimates the contribution to fluorescence in the absence of oleic acid. These experiments were run at different concentrations of oleic acid and at a fixed protein−fluorophore concentration.

Circular Dichroism. Spectra were recorded on a JASCO J-20 spectropolarimeter employing cuvettes connected to a circulating water bath (Haake). The temperature of the sample was measured directly into the cuvette with the aid of an electronic thermocouple. Spectra in the near UV region (250−450 nm) or in the far UV region (200−250 nm) were collected using either a 50 or a 1 mm path cuvette, respectively, closed with Teflon caps. The scanning speed was 10 nm/min and the time constant 1 s. Each sample was scanned four times, and the data were averaged to reduce noise. Increasing amounts of ANS or bisANS were added to a solution of 20 μM IFABP in buffer A, and spectra were recorded at the corresponding temperature. In addition, the spectrum of a solution of IFABP incubated with each of the probes was measured as a function of temperature in both UV regions. Molar ellipticity was calculated as described elsewhere (*23*).

Limited Proteolysis. Clostripain (Arg-C, Promega) was activated by incubation in 20 mM Tris-HCl, pH 7.8, 50 mM NaCl, and 1 mM DTT for 1 h prior to its use. Digestion with this enzyme of native IFABP (0.5 mg/mL) dissolved in the same buffer was carried out at 37 °C for the periods indicated. The ratio of protein to protease was 20:1 (w/w), unless otherwise stated. Apo-IFABP, holo-IFABP (bound to oleic acid), ANS-IFABP, or bisANS-IFABP were incubated at the same temperature for 15 min before the protease was added. At fixed intervals, samples were separated, mixed with sample buffer (0.005% (w/v) bromophenol blue, 4% (w/v) SDS, 10% (v/v) glycerol, 15% (v/v) 0.33 M Tris-HCl, pH 6.8, 2% β-mercaptoethanol), heated for 5 min at 100 °C, and analyzed by SDS−PAGE (*24*). The composition was 4% T, 3% C for stacking and 16.5% T, 3% C for running gels. 30 V were applied at the beginning of the run until the sample reached the running gel, then the voltage was raised to 90 V. Gels were stained with 0.1% (w/v) colloidal Coomassie Brilliant Blue G dissolved in 2% (v/v) H_3PO_4, 15% (w/v) $(NH_4)_2SO_4$ during 2 h, and destained with a methanol/acetic acid/water solution (15:15:70, v/v). Digital images were collected by placing the gel between two glass plates in a scanner connected to a PC. The pattern of bands was analyzed using SigmaGel 1.0 software. After that, gels were dried under vacuum before storage.

Peptide Sequencing. Following electrophoresis, the resulting fragments were transferred to a PVDF membrane (Immobilon-P) under semi-dry conditions (*25*). Blotting conditions were 1 h of transfer at room temperature under constant current (80 mA). The membrane was then stained by immersing it in 0.1% (w/v) Coomassie Brilliant Blue R in 50% (v/v) methanol for 5 min and destained with aqueous solutions of increasing methanol concentration (10−50%, v/v). The bands of interest were cut and submitted to Edman degradation at the local protein sequencing facility.

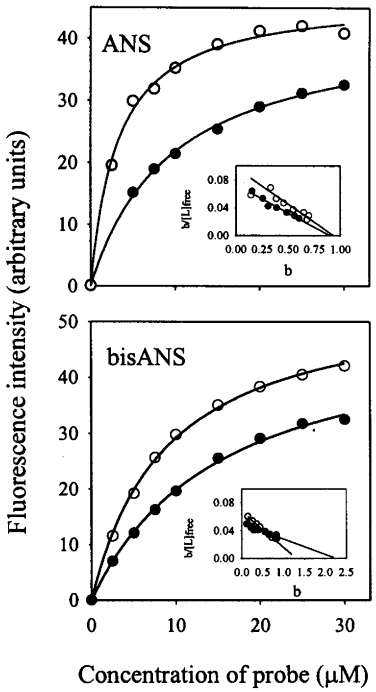

FIGURE 1: Titration of IFABP with fluorescent probes**.** IFABP (2 μM) was titrated with ANS or bisANS at 28 °C (empty circles) or 39 °C (filled circles). Increasing amounts of the ligand were added to the protein solution, and the fluorescence intensity was measured after equilibration of the sample for 2 min. Excitation wavelength was 400 nm, and the emission was monitored at 480 or 490 nm for ANS or bisANS, respectively. The solid lines correspond to the optimal curve fitting of the data by nonlinear regression to eqs 1 or 3, respectively (see Materials and Methods). The insets show the corresponding Scatchard plots (eq 2).

Molecular Exclusion Experiments. A Superdex HR-75 FPLC column (Pharmacia) was equilibrated in 20 mM potassium phosphate buffer, 100 mM NaCl. Elution of this column was carried out at 28 or 40 °C at a flow rate of 0.75 mL/min. Samples (500 μL) containing apo-IFABP (0.5 mg/mL) or IFABP in the presence of bisANS (incubated at the corresponding temperature at a molar protein/ligand ratio of 1:2) were loaded onto the column. Elution was monitored at 220 nm, and the protein peaks were collected. Their fluorescence emission at 480 nm (excitation at 380 nm) was also evaluated.

RESULTS

Binding of the Fluorescent Probes ANS and bisANS to IFABP. Titration Experiments. Fluorescence measurements in the presence of the extrinsic probes ANS or bisANS were carried out to obtain information on the conformational change that IFABP undergoes in the temperature range of 35−50 °C. The quantum yield of each fluorophore increases dramatically from the aqueous solutions (0.003 and 0.001 for ANS and bisANS, respectively) to their bound states (0.2 and 0.38 for ANS and bisANS, respectively).

To characterize the binding activity of ANS and bisANS to IFABP, titration assays were performed at 28 °C, a temperature below the transition, and at 39 °C, a temperature within the transition range (Figure 1). The center of mass of

Table 1: Binding Parameters Obtained by Nonlinear Regression of Data from Figure 1

	ANS		bisANS	
	28 °C	39 °C	28 °C	39 °C
n	1.0 ± 0.1	0.9 ± 0.2	1.3 ± 0.1	2.2 ± 0.5
K_d (μM)	3.2 ± 0.2	9.6 ± 0.5	8.8 ± 0.4	15.5 ± 1.0

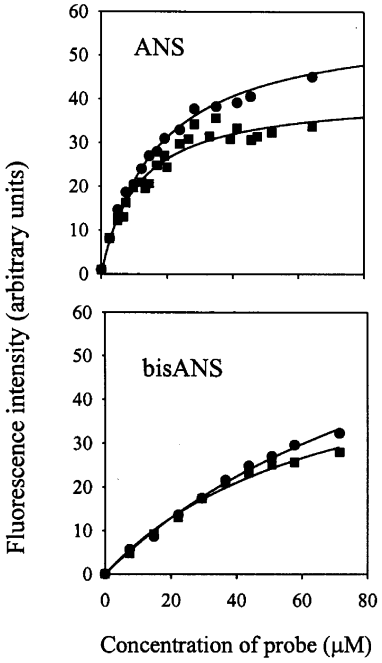

FIGURE 2: Effect of ionic strength on the binding of the fluorescent probes to IFABP. IFABP (2 μM) was titrated at 39 °C with ANS or bisANS in an extended range of concentration at low (buffer A: circles) or high ionic strength (buffer A supplemented with NaCl up to 0.24 M final concentration: squares). Fluorescence was monitored under the same conditions as those described for Figure 1. The solid lines correspond to the optimal curve fitting of the data by nonlinear regression to models of one site or of two nonidentical and noninteracting sites (eqs 1 or 3, for ANS or bisANS, respectively).

the fluorescence spectra of free ANS and bisANS in aqueous or organic (ethanol) solution does not vary with temperature (518.0 ± 1.1 and 530.1 ± 0.6 nm for ANS and bisANS, respectively, in water and 480.9 ± 0.4 and 494.2 ± 0.1 nm for ANS and bisANS, respectively, in ethanol). A shift to lower wavelengths occurs upon binding of these probes to IFABP (490 and 500 nm for ANS and bisANS, respectively), as expected from the more hydrophobic protein environment around these probes in their bound forms.

Both ANS and bisANS showed dissociation constants (K_d) in the micromolar range (Table 1). The binding parameters K_d and n, the number of ligand molecules bound to IFABP, were calculated by the titration procedures described in Materials and Methods.

In accordance to previously published results (*26*), the binding stoichiometry of IFABP/ANS is 1:1 at both temperatures. Under our experimental conditions, at concentrations of ANS in the range of 60−100 μM, an additional low affinity site appears (K_d = 198 ± 60 μM), as evidenced by the fitting of the data by nonlinear regression to a model of two nonidentical and noninteractive sites (Figure 2). Nevertheless, this low affinity binding site disappears when the ionic strength is increased (at 0.24 M NaCl, Figure 2),

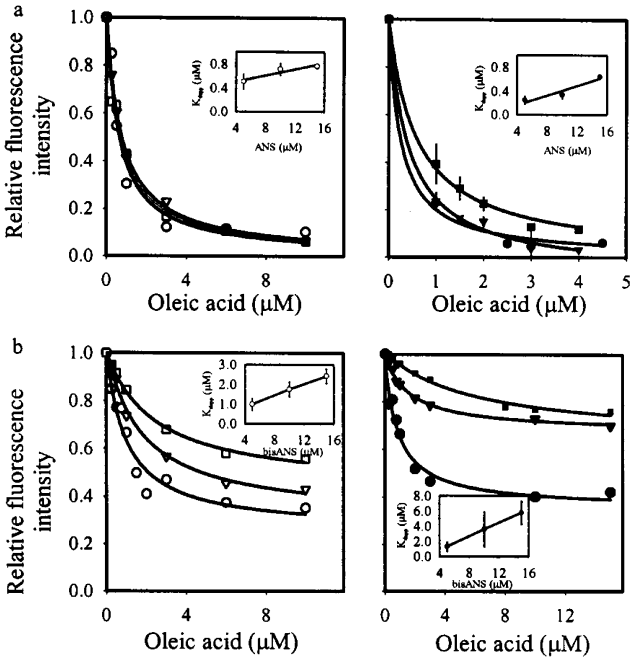

FIGURE 3: Competition of the fluorescent probes bound to IFABP by oleic acid. ANS (a) or bisANS (b) bound to IFABP were incubated with increasing amounts of oleic acid at 28 °C (empty symbols) or 39 °C (filled symbols). The relative fluorescence intensity equals the ratio between the fluorescence measured in the presence of a given amount of oleic acid and that in its absence. At each temperature assayed, IFABP (2 μM) dissolved in buffer A was incubated with each probe at 5 μM (circles), 10 μM (inverted triangles), or 15 μM (squares) final concentration. Increasing amounts of oleic acid in the same buffer were added next, and the fluorescence intensity was measured after equilibration of the sample for 2 min. The continuous lines are the best fit to the data of eq 5 by nonlinear regression. The insets show the dependence of the apparent dissociation constant for oleic acid (K_{dapp}) obtained after the fitting procedure described above as a function of the fluorescent probe concentration (see text for details).

whereas the high affinity site exhibits a somewhat higher dissociation constant (21.8 ± 6.9 μM).

In the case of bisANS, the binding stoichiometry is close to 1:1 at 28 °C (Table 1), and it does not change up to 100 μM bisANS. By contrast, at 39 °C a second site appears with a value of K_d indistinguishable from the first (Figure 1). At variance with ANS, this second site persists in the presence of 0.24 M NaCl (Figure 2). As far as we were able to evaluate by direct absorption and fluorescence spectra, no noticeable change in light dispersion occurs upon addition of any of the probes to an IFABP sample.

Competition Experiments. Competition experiments were performed to investigate whether the fluorescent probes bind to the fatty acid binding site. Previous work on different iLBPs, including IFABP (*27*, *28*), showed that ANS is displaced by many fatty acids, suggesting that this ligand occupies the same binding pocket. We conducted a similar experiment at 28 and 39 °C using oleic acid as the competitor. In addition, the binding of bisANS was also studied comparatively. Figure 3a shows that ANS is completely displaced by oleic acid at both temperatures assayed. A linear dependence of K_{dapp} with ANS concentration suggests a simple competitive behavior (see insets), although this trend is barely apparent, precisely as one would expect for a ligand showing much less affinity than the natural one. To underscore this point, note that $K_{dapp} = K_o + [L](K_o/K_d)$,

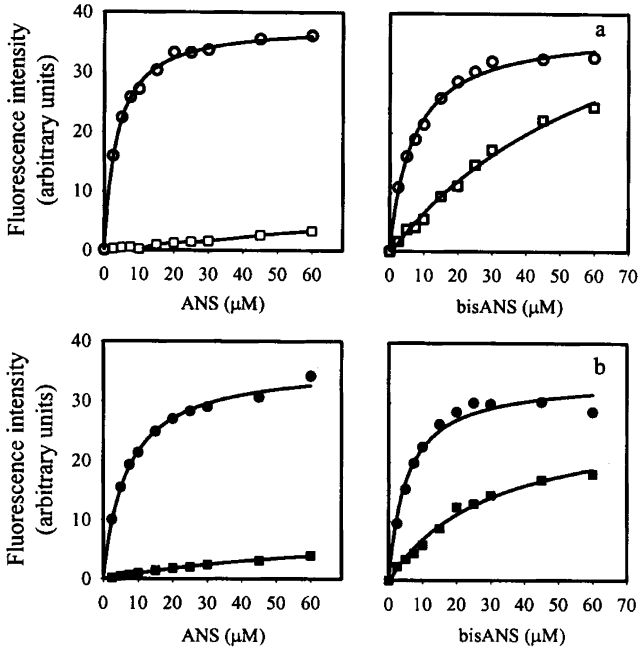

FIGURE 4: Effect of a saturating concentration of oleic acid on the binding of the fluorescent probes to IFABP. IFABP (2 μM) was titrated with ANS or bisANS in the presence (squares) or in the absence (circles) of a saturating level of oleic acid (8 μM) at 28 °C (a) or at 39 °C (b). In the presence of oleic acid, the values of K_d for bisANS after fitting eq 1 to the data were 81.0 ± 15.8 and 32.1 ± 4.8 μM at those temperatures, respectively.

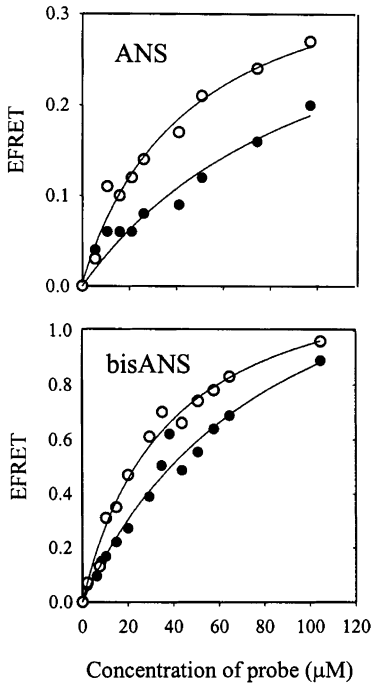

FIGURE 5: Titration of IFABP with fluorescent probes by FRET. IFABP (2 μM) was titrated with ANS or bisANS at 28 °C (empty circles) or 39 °C (filled circles), and the efficiency of FRET (EFRET) was monitored (see eq 6 in Materials and Methods). Increasing amounts of the fluorescent ligand were added, and after 2 min equilibration, the fluorescence intensity integrated in the range of 310−400 nm was collected (I_{da}). Excitation wavelength was 290 nm. The continuous lines correspond to the optimal curve fitting of eqs 1 or 3 to the data by nonlinear regression, as indicated in Figure 1.

where [L] is the concentration of the fluorescent probe, and K_o and K_d are the dissociation constants for oleic acid and the fluorescent ligand, respectively.

On the other hand, bisANS is only partially displaced at 28 and 39 °C, albeit to a different extent (i.e., the most remarkable feature being that a remnant fluorescence is observed that cannot be attributed to an enhancement effect occurring in the presence of oleic acid). This behavior increases both with bisANS concentration and temperature (Figure 3b). The temperature-induced additional binding site appears superimposed to another one showing a competitive binding mode similar to that observed for ANS (inset), in agreement with results from titration experiments (Figure 1).

We investigated whether the observed remnant fluorescence appears as a consequence of covalent binding of bisANS to IFABP through a photochemical reaction. In this regard, Seale et al. (*29*, *30*) showed that bisANS can covalently attach to sites in the chaperonin GroEL if irradiated under certain circumstances. To investigate this matter further, we incubated bisANS with IFABP under three different conditions: the first sample was kept in the dark, a second one was handled as is routinely done to measure its fluorescence, and the third one was irradiated on purpose for 10 min with light from a 366 nm UV source. After these treatments, all samples were exhaustively dialyzed against buffer A to free them of any noncovalently bound bisANS before measuring their fluorescence. Only the sample that had been purposely irradiated showed significant fluorescence (50% of the initial fluorescence). Conversely, under usual illumination bisANS does not become covalently bound to the protein (less than 6%).

With the aim of revealing the binding site exclusive for bisANS, we decided to carry out titration experiments similar to those described above but in the presence of a saturating concentration of oleic acid (Figure 4). Given the known values of K_d for the fluorescent ligands (refs *26*, *31*, *32*, and this paper) a maximal ratio of fluorescent probe to oleic acid of 6:1 was estimated to be enough to prevent the displacement of the fatty acid from its binding site. Under these conditions, at both temperatures assayed the fluorescence intensity of ANS remains negligible up to 60 μM, confirming that this ligand shares the same binding site with oleic acid. Conversely, the fluorescence intensity of bisANS increases significantly in the same range of concentration, either at 28 or at 39 °C.

FRET Analysis. A significant overlap between the emission spectrum of IFABP and the absorption spectrum of ANS or bisANS allowed us also to monitor the binding of these fluorophores by FRET. Titration curves of IFABP with ANS or bisANS were carried out by excitation of the sample at 290 nm. FRET was evidenced by a decrease in the fluorescence intensity in the range of 310−400 nm. A concomitant increase was observed of the fluorescence intensity in the range of 400−600 nm (not shown).

There is a close correspondence between the titration curves estimated by the measurement of the efficiency of FRET (EFRET) and by direct excitation of the ligands (cf. Figures 5 and 1). The fitting of the data to the binding models described in Materials and Methods rendered values of K_d equal to 6.1 ± 1.9 μM at 28 °C and 22.9 ± 14.0 μM at 39 °C for ANS, and 16.4 ± 1.2 μM at 28 °C and 21.1 ± 11.3 μM at 39 °C for bisANS.

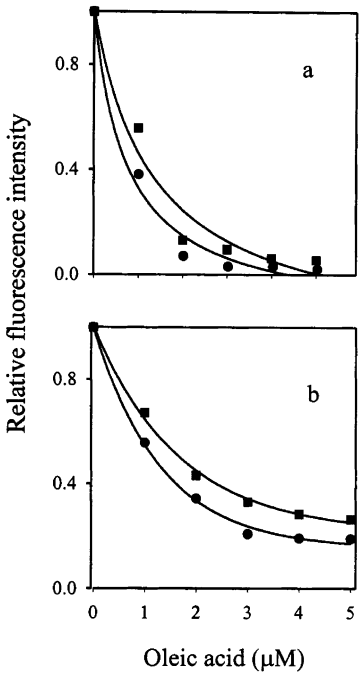

FIGURE 6: Competition of fluorescent probes bound to IFABP by oleic acid as monitored by FRET. ANS (a) or bisANS (b) bound to IFABP was incubated with increasing amounts of oleic acid at 39 °C. This assay was run at two different probe concentrations: 5 μM (circles) and 15 μM (squares). The relative fluorescence intensity equals the ratio between the EFRET observed at 480 or 495 nm (for ANS or bisANS, respectively) in the presence of a given amount of oleic acid and that measured in its absence. Excitation wavelength was set at 290 nm. The continuous lines correspond to the nonlinear regression fitting of eq 5 to the data. The values of K_{dapp} (μM) estimated after this procedure were 0.35 $\pm$ 0.12 (5 μM ANS); 0.61 $\pm$ 0.22 (15 μM ANS); 1.04 $\pm$ 0.10 (5 μM bisANS); and 2.10 $\pm$ 0.20 (15 μM bisANS).

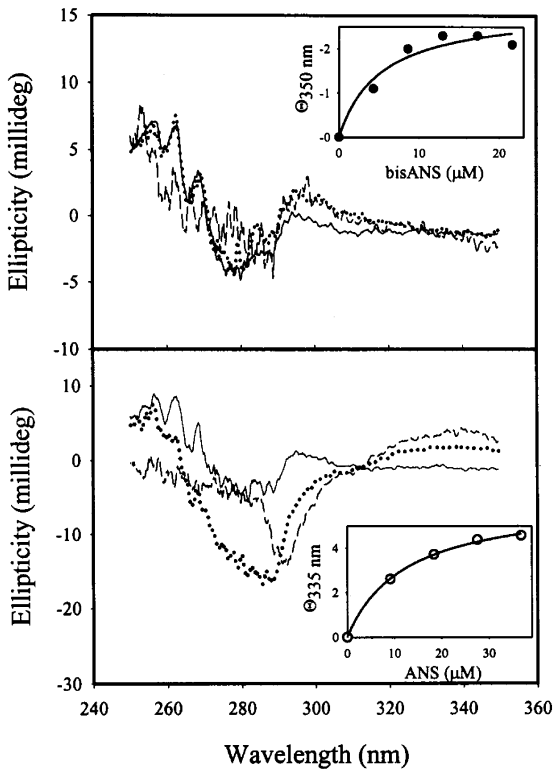

FIGURE 7: Near UV circular dichroism spectra of IFABP bound to the fluorescent probes. The spectrum of IFABP (20 μM, continuous line) and those of samples incubated with ANS (lower panel) or bisANS (upper panel) at 39 °C at two different concentrations of probe (9.2 μM, dotted line and 36.8 μM, dashed line) are shown. The insets show the evolution of the ellipticity signal at selected wavelengths (335 or 350 nm for ANS or bisANS, respectively) as a function of fluorescent probe concentration at 39 °C. The continuous lines correspond to the nonlinear regression fitting of the data to eqs 1 or 3 (see Materials and Methods). The values of K_d obtained by this method were 12.5 $\pm$ 1.2 μM for ANS and 5.2 $\pm$ 2.5 μM for bisANS.

Next, we analyzed EFRET data of competition assays with oleic acid. Here, we decided to measure instead the fluorescence enhancement at 480 or 495 nm for ANS or bisANS, respectively (Figure 6) because the binding of oleic acid produces an increase in the intrinsic fluorescence intensity of IFABP that opposes the expected fluorescence decrement because of energy transfer. For each fluorophore, the apparent dissociation constant for oleic acid (K_{dapp}) was estimated according to eq 5 (see Materials and Methods) from the measurement of the decrease in fluorescent intensity at the corresponding wavelength after the addition of varying amounts of oleic acid to an IFABP-probe solution. In close agreement with the competition assays shown in Figure 3, at 39 °C the fluorescence intensity because of bound ANS approaches zero as oleic acid is added. By contrast, an asymptotic value significantly different from zero is observed in the case of bisANS. This remnant fluorescence increases slightly at a higher concentration of bisANS. The apparent dissociation constants derived in this fashion were similar to those found by the direct measurement of the fluorescence of these probes (cf. Figures 3 and 6). As regards the nondisplaceable binding site observed for bisANS, the results above suggest that its location should lie within the boundaries imposed by the values of R_o for the pair IFABP−bisANS (see Materials and Methods).

Circular Dichroism. Binding of ANS to IFABP induces a positive band centered at 335 nm that increases with ANS concentration (Figure 7, lower panel; see also Figures 9 and S3, Supporting Information). This band corresponds to bound ANS given that the protein does not show any significant signal around this wavelength region. There are other bands that change their intensity in the range of 250−300 nm, but they represent a mixed contribution of IFABP aromatic transitions and the induced bands of the probe. Titration of IFABP with ANS rendered a similar K_d (12.5 $\pm$ 1.2 μM) to that measured by fluorescence methods (Figure 7, inset). Similarly, binding of bisANS to the protein induces a negative band centered at 350 nm, which arises as a consequence of the bound fluorophore (Figure 7, upper panel, see also Figures 9 and S3, Supporting Information). Following this signal in a titration assay, we calculated a value for a K_d of 5.2 $\pm$ 2.5 μM, which also agrees well with that already obtained by fluorescence measurements (Figure 1). As mentioned in the introductory paragraphs, bisANS, but not ANS, was able to reveal the thermal transition of IFABP (*12*). Here, we investigated this matter further by monitoring the CD spectrum of IFABP complexed to each probe as a function of temperature. When the probes are bound to IFABP, the dichroic signal in the far UV region hardly changes up to 75 °C, a temperature at which the onset of unfolding occurs (Figure 8). Although there is a decrease in the absolute value of the molar ellipticity at 215 nm (amounting to about 1000 deg cm^2 dmole^{-1}) from free IFABP to IFABP bound to bisANS, this phenomenon is not

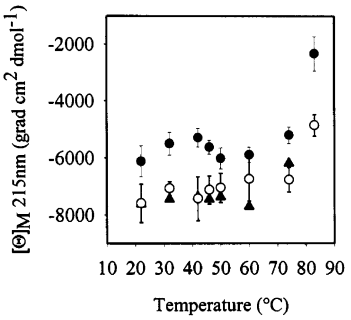

FIGURE 8: Evolution of the molar ellipticity at 215 nm of IFABP (triangles) and those of samples incubated with ANS (empty circles) or bisANS (filled circles) as a function of temperature. Protein/probe molar ratio was 1:8.

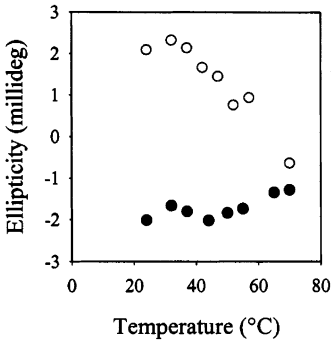

FIGURE 9: Evolution of the ellipticity signal at 335 or 350 nm for ANS (empty circles) or bisANS (filled circles), respectively, bound to IFABP as a function of temperature. Protein/probe molar ratio was 1:8.

observed for bound ANS. On the other hand, the ANS-induced dichroic signal at 335 nm decreases with increasing temperature in agreement with the expected amount of remaining complex, as calculated on the basis of the variation of the dissociation constant in the same temperature range (Figure 9). By contrast, the corresponding bisANS signal does not change significantly with temperature. These results point to the different binding nature of these ligands, a phenomenon already observed in the fluorometric assays.

Limited Proteolysis. Partial proteolysis can shed light on the location of ligand binding sites or conformational changes in proteins since this technique reveals the differential exposure of proteolytic sites. We investigated the peptide pattern arising from IFABP after digestion with clostripain (Arg-C), in the absence or in the presence of oleic acid, ANS, or bisANS (Figure 10). This enzyme hydrolyses the polypeptide chain at the C-terminal end of arginine residues. The performance of limited proteolysis at different temperatures brings about the complication of the influence of this variable on the activity of clostripain. For this reason, assays were performed only at 37 °C, which is the optimal temperature for the proteolytic activity of this enzyme.

Only quantitative differences were evident between the apo-protein and the complexes with the ligands (Figure 10). From the time course of proteolysis, maximal differences occur at 40 min. IFABP shows the highest level of protection from proteolysis when bound to oleic acid, as compared to the other samples. The digestion pattern of IFABP−ANS complex resembles closely that shown by the apo-protein, whereas the bisANS−IFABP complex is proteolyzed more rapidly, as evidenced by a marked decrease in the band corresponding to native IFABP.

The proteolytic fragments of the protein observed in the presence of ANS and an excess amount of oleic acid rendered the same pattern as that seen for holo-IFABP, a result in agreement with the expected full displacement of ANS by the fatty acid (cf. lanes 3 and 5, Figure 11). Unlike ANS, the pattern obtained when IFABP is proteolyzed in the presence of bisANS and an excess amount of oleic acid differs from that of the holo-protein, most predominantly, since the relative abundance of the 11 K band is increased (cf. lanes 3 and 7, Figure 11). These results suggest a different binding mode for this ligand, a fact consistent with the existence of a second binding site for bisANS.

To test whether any direct effect of the ligands exists on the enzymatic activity, after incubation of IFABP with each of these molecules and previous to the addition of the enzyme, samples were freed from remaining ligands by filtration in Microcon tubes. After this treatment, in all cases the peptide patterns obtained were indistinguishable from those described above (data not shown). In addition, we assayed the proteolysis of two unrelated proteins in the presence of bisANS:bovine serum albumin and bovine α-lactalbumin. In any of these cases, this ligand did not enhance the degradation of the proteins, indicating that bisANS by itself does influence the protease activity of clostripain (data not shown).

After electroblotting, the two main fragments generated from IFABP corresponding to the 11 and 8 K bands were submitted to Edman degradation. Both fragments rendered

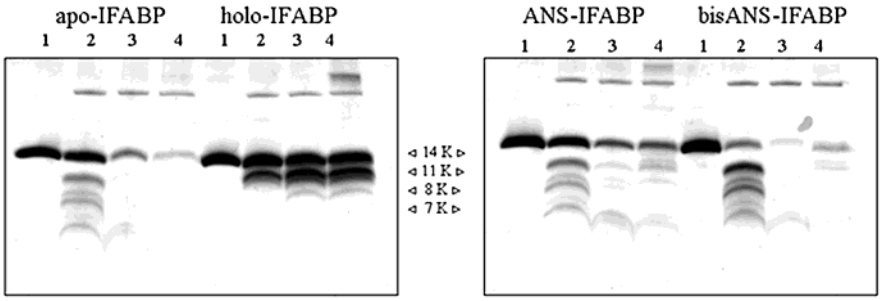

FIGURE 10: Time-course of proteolysis of free IFABP and IFABP bound to ligands. Delipidized IFABP (apo-IFABP, 0.5 mg/mL) and samples of this protein preincubated for 15 min at 37 °C with a saturating concentration of oleic acid (holo-IFABP), ANS (ANS-IFABP), or bisANS (bisANS-IFABP) were submitted to proteolysis with clostripain. The ratio of protein to protease was 20:1 (w/w). Samples were taken at 40 (lanes 2), 120 (lanes 3), and 240 min (lanes 4). Lanes 1 correspond to samples taken before the addition of the enzyme. Immediately thereafter, samples were separated by SDS−PAGE, and the gels were stained with colloidal Coomassie Brilliant Blue as indicated in Materials and Methods. The approximate relative molecular mass of the major proteolytic fragments is indicated.

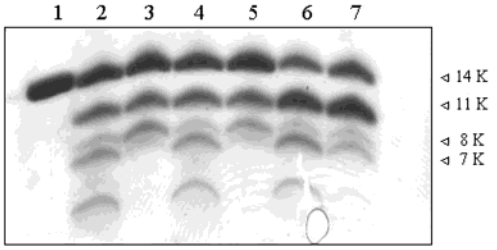

FIGURE 11: Effect of a saturating concentration of oleic acid on proteolysis of IFABP. Separation by SDS−PAGE of proteolytic fragments of apo-IFABP (lane 2), holo-IFABP (lane 3), ANS-IFABP (lane 4), ANS-IFABP incubated with an excess amount of oleic acid (lane 5), bisANS-IFABP (lane 6), and bisANS-IFABP incubated with an excess amount of oleic acid (lane 7). Lane 1 corresponds to undigested IFABP. Proteolysis with clostripain was carried out at 37 °C for 40 min. Gels were stained with colloidal Coomassie Brilliant Blue as indicated in Materials and Methods. The relative molecular mass of the major proteolytic fragments is indicated.

the same N-terminal sequence (KLGAH), indicating a cleavage at arginine 28. This residue belongs to helix II, a structure that is part of the entry portal region. The different accessibility of the protease to this particular site underscores a dynamic role played by this domain.

Exclusion Chromatography. Given that an enhanced binding of bisANS or ANS has usually been associated to the molten globule state of a protein, we choose molecular exclusion chromatography as an alternative tool to investigate whether the conformational state described above for the bisANS−IFABP complex could bear any similarity to a molten globule. For this purpose, IFABP incubated with bisANS was sampled on a Superdex HR-75 column and run at 28 or 40 °C. Results from these chromatograms were compared with a control sample of apo-IFABP. Elution profiles are indistinguishable: a single symmetric peak of similar width is observed in all cases, a result consistent with a compact well-folded state (Figure S4, Supporting Information).

In addition, the ligand bisANS was found to be associated to the protein peak: ~25% of the fluorescence originally present in a mixture of bisANS and IFABP sampled into the column (after correcting by dilution). A separate sample of bisANS and IFABP incubated in the presence of oleic acid shows a similar level of fluorescence coeluting with the protein (data not shown). This behavior agrees with results from fluorescence experiments shown before and points to the persistence of a second binding site for bisANS in this protein.

DISCUSSION

Fluorescent Probe bisANS−Unlike ANS−Reveals a Temperature-Induced Binding Site in IFABP. ANS and bisANS bind to IFABP with similar affinity (Figure 1 and Table 1). The bisANS molecule is a covalent dimer of ANS linked directly through the naphthalene moieties (see Scheme 1). Unlike other double ligands, which show a dramatically increased affinity as compared to that exhibited by the monomeric species (see, i.e., refs *33* and *34*), bisANS fails to do so in this case. Nevertheless, a structural distinction should be pointed out: the presence of a covalent linker long enough to allow independent interaction at distinct binding sites is missing in this compound. On the other hand, the values of K_d reported in this study are comparable to those measured for other native proteins that bind these same ligands but differ from the lower affinity ($K_d \geq 0.1$ mM) generally observed for folding intermediate states (for a comprehensive table see ref *35* and references therein).

Estimates of K_d obtained by the measurement of different fluorescence parameters, namely, fluorescence intensity and EFRET (see Figures 1 and 5) or by independent methods, such as fluorescence and circular dichroism (see also Figure 7), agree well. On the other hand, the measured binding stoichiometry is 1:1 for ANS at the temperatures assayed, in accordance with results from other authors (*26*). Consistent with this evidence, NMR data on ANS complexed to IFABP shows a single binding site for this ligand (*36*). Conversely, and as shown in Figure 1 and Table 1, in the case of bisANS a second binding site with a similar affinity for this ligand appears at a higher temperature (39 °C). At high ANS concentration, a second site with a higher K_d (~200 μM) appears, but binding to this site can be prevented by increasing ionic strength (Figure 2a). By contrast, binding of bisANS to the second site persists even at high ionic strength (Figure 2b), thus ruling out nonspecific electrostatic interactions as the source of the additional binding observed for the latter.

Experiments employing the natural ligand oleic acid as a competitor showed that ANS is completely displaced by the fatty acid at all temperatures assayed, indicating that this probe is located within the binding cavity of IFABP (Figure 3a). By contrast, bisANS is only partially displaced by oleic acid, as evidenced by the remnant fluorescence observed at high oleic acid concentration (Figure 3b). This effect is more notorious as the temperature is raised from 28 to 39 °C. Since residual fluorescence was observed by other authors because of photo-cross-linking of bisANS to proteins (e.g., with chaperonin GroEL: refs *29* and *30*), we investigated whether this could have happened in our case. In the end, we ruled out this possibility after comparing the negligible fluorescence observed in a sample that had been handled under usual illumination conditions with that of a sample that had been purposely irradiated at 366 nm with a UV lamp source. In view of this fact, our interpretation holds that bisANS is indeed interacting noncovalently with an additional binding site to IFABP.

Further support for a second binding site for bisANS was provided by the titration of IFABP with this fluorescent probe in the presence of a saturating concentration of oleic acid (Figure 4). Control experiments were run alongside with ANS. As expected, ANS fluorescence enhancement is negligible in an extended range of concentration, indicating once again that this ligand most likely occupies a site within the binding cavity of IFABP common to that observed for the fatty acid. Conversely, bisANS fluorescence intensity increases in the same range, even under conditions where the fatty acid binding site is fully occupied by oleic acid. The good agreement between these last assays with the results shown earlier (Figure 3) eliminates any kinetic barrier associated with the entry or exit of the ligands as the origin of the peculiar features observed for bisANS binding.

Accordingly, the FRET experiments also support these results. Competition of each fluorophore with oleic acid exhibited parallel behaviors to those observed for the direct excitation of the ligand (i.e., in the case of bisANS at 39

°C, there is evidence for energy transfer, even at saturating concentrations of oleic acid), whereas the FRET efficiency becomes drastically reduced if ANS is the acceptor. In the former case, the extent of remnant fluorescence intensity is different from the level observed in the direct excitation experiment. Nevertheless, the distinct nature of each process might account for the differences observed: (i) the quantum yield of bound ligands to different sites might not necessarily be identical and (ii) uncertainties exist associated with the distance and/or orientation of the donor tryptophan and the acceptor ligand in FRET experiments.

In the presence of an excess amount of any of the fluorescent ligands, the shape of the CD spectrum in the far UV region is overall maintained, although for bisANS a positive difference (~14%) exists centered at around 215 nm (Figure S2, Supporting Information). In principle, this feature could be attributed either to an induced signal of bisANS in its bound form or to a disturbance of the secondary structure of IFABP arising as a consequence of bisANS binding. In this regard, other authors have reported conformational changes on proteins induced by bisANS binding (*35*, *37*, *41*). However, this seems unlikely in our case given that the CD spectrum in the range of 250−300 nm of the protein bound to bisANS retains its characteristic fine structure. For bisANS bound to IFABP, the induced band at 215 nm does not appear to change significantly in the temperature range assayed (Figure 8), a circumstance that could arise as a result of compensatory causes (i.e., loss of affinity versus appearance of a new binding site), as will be discussed below. On the other hand, the ability to detect subtle changes in this spectral region is hampered by the overwhelming magnitude of signals corresponding to secondary structure. Therefore, we extended this analysis to the near UV regions.

In the UV range of 250−410 nm, induced bands indeed appear because of the binding of ANS or bisANS to IFABP. For ANS, the presence of defined isodichroic points indicate that the observed spectral changes reflect simply the binding of the fluorescent ligand to the protein, a phenomenon that does not imply an alteration of the protein scaffold. By contrast, this spectral feature is not apparent for bisANS, especially in the region of 250−320 nm, giving rise to the possibility that the ligand might also induce conformational changes upon binding to the protein (see discussion below). Specifically, the signals that appear in the range of 310−410 nm can be unambiguously used to monitor the binding of the probe given that the protein does not contribute ellipticity in this range. In this fashion, we performed titration assays to calculate the value of K_d for each probe (insets to Figure 7). On the other hand, we studied the behavior of each main signal (those at 325 and 350 nm, for ANS and bisANS, respectively) as a function of temperature (Figure 9). Our interest in this matter originated in previous results from fluorescence measurements (see Figure 6 in ref *12*), where we had detected a thermal transition in IFABP by following the fluorescence intensity of bisANS bound to the protein. In this study, we could also observe a different behavior between ANS and bisANS bound to IFABP: the magnitude of the ANS-induced dichroic signal decreases with increasing temperature, whereas the corresponding signal of bisANS suffers little change (Figure 9). A plausible explanation is that ANS dissociates from the protein as temperature increases according to the known thermodynamic dependence of K_d with this parameter (*27*). A numerical simulation of this equilibrium yields a trend that agrees well with the experimental measurements (results not shown). Conversely, the anomalous behavior of bisANS (i.e., the only minor variation of the CD signal for bisANS−IFABP) rather than the expected decrease in the signal because of a lesser affinity (Table 1) most likely result from a compensatory phenomenon because of the appearance of an additional binding site.

bisANS Bound to IFABP Unveils an Alternative Conformational State of this Protein. With the aim at searching for a possible structural correlation with the observed spectral changes, we inspected IFABP conformation by differential susceptibility to proteolysis. The results derived from digestion with clostripain indicate the following:

(i) Holo-IFABP is the most resistant species, a fact consistent with a closed conformation analogous to that observed for three related proteins (CRBPs types I and II and HFABP, ref *9*) analyzed by this same technique, and which might possibly correspond to the ordered conformation proposed by Hodsdon and Cistola on the basis of NMR data (*7*, *8*).

(ii) The ANS−IFABP complex behaves similarly to the apo-structure, showing that the location of this ligand within the β-barrel fails to protect the entry portal region from proteolysis.

(iii) By contrast, the bisANS−IFABP complex turned out to be the most labile species to cleavage by clostripain. This might suggest an interaction of this ligand with the helical domain that favors the presentation of the proteolytic site, either by increasing its exposure or by changing the protein surface charge. In this regard, there is evidence that bisANS induces a conformational change in DnaK by preferentially binding to its partially folded intermediate state, thus stabilizing this conformation (*35*). Nevertheless, in our case, values of K_d found for bisANS are comparable to those measured for other proteins that bind amino naphthalene sulfonates in their native state (*35*). On the other hand, bisANS does not appear to significantly change the hydrodynamic properties of IFABP, as ascertained by size exclusion chromatography (not shown), a behavior consistent with a compact well-folded state. From a structural standpoint, given that the positively charged helical domain of IFABP might interact electrostatically with bisANS, we cannot rule out the possibility that binding of this ligand by itself might influence proteolytic activity. An alternative explanation to the enhanced proteolysis could be the direct binding of this fluorophore to clostripain and the concomitant change in its activity. However, a similar experiment using bovine serum albumin or α-lactalbumin showed that bisANS protects these proteins from cleavage, opposite to what is observed with IFABP, thus ruling out an effect on the protease (data not shown).

(iv) The addition of an excess amount of oleic acid to the ANS−IFABP complex yields a proteolytic pattern indistinguishable from that of holo-IFABP (cf. lanes 3−5 in Figure 11), in agreement with the already observed full displacement of this fluorescent probe (Figure 3a), while under the same experimental conditions, the pattern obtained for the sample containing bisANS−IFABP deviates from that of the holoprotein (cf. lanes 3, 6, and 7 in Figure 11). Sequencing of the 11 K fragment reveals a cleavage at arginine 28. This

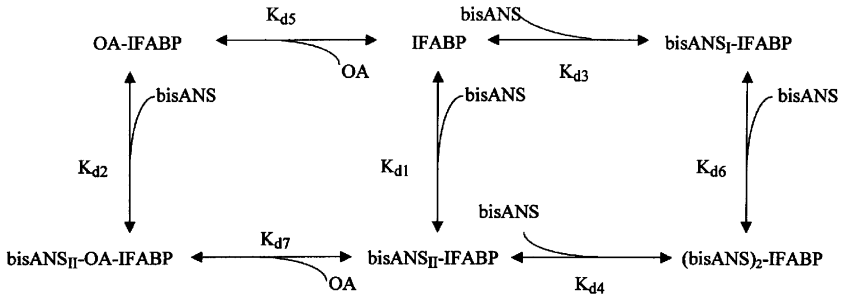

FIGURE 12: Model proposed for the interaction of bisANS and oleic acid with IFABP. IFABP is the apo-protein; OA-IFABP represents the protein bound to oleic acid (holo-IFABP); $bisANS_I$-IFABP represents the complex between the protein and the bisANS bound to site I (the site shared with oleic acid); $bisANS_{II}$-IFABP is the complex where bisANS is bound to its exclusive site (site II); and $(bisANS)_2$-IFABP and $bisANS_{II}$-OA-IFABP denote the ternary complexes. $K_{d1}-K_{d7}$ are the dissociation constants for each binding step. A simulation of the experimental behavior shown in Figures 3b and 4 yields the following values for the dissociation constants: $K_{d1} \sim K_{d3} \sim K_{d4} \sim 5\ \mu M$, $K_{d2} \sim 50\ \mu M$, and $K_{d5} \sim 0.2\ \mu M$ at 28 °C; and $K_{d1} \sim 2.5\ \mu M$, $K_{d3} \sim K_{d4} \sim 7.5\ \mu M$, $K_{d2} \sim 30\ \mu M$, and $K_{d5} \sim 0.4\ \mu M$ at 39 °C.

residue is located in helix II of IFABP, a site belonging to the entry portal region for the fatty acid ligand. Protection from proteolysis at this very same site was also found for other members of the family of lipid binding proteins (i.e., CRBPs I and II, and HFABP when bound to their natural ligands (*9*)).

According to the dynamic portal hypothesis, the fatty acid enters the binding cavity in IFABP through a locally disordered region that involves the C-terminal half of helix II, the linker αII/βB, and the turns between strands βC-βD and βE-βF. This feature characterizes the so-called open conformation revealed by NMR studies (*6*−*8*). Once the fatty acid is bound, it would stabilize an ordered conformation (closed form) through a series of cooperative interactions similar to those occurring at the C-terminal capping box motif, a structural motif localized at the end of a helix that involves the hydrogen atoms of amides and the oxygen atoms belonging to the backbone of the protein that do not participate in the hydrogen bonds of the helix. The release of the fatty acid would be catalyzed by any process that destabilizes the helix-capping, such as collisions with phospholipid membranes (*37*). In this regard, a study of a helixless variant of IFABP provided kinetic evidence of a rate-limiting step for the ligand binding reaction implicating a conformational change at the helical domain (*38*). Nevertheless, this domain is not essential for preserving the integrity of the fatty acid binding cavity, but it might instead contribute to regulate the affinity of the protein for different fatty acids. Results from spectroscopic measurements and limited proteolysis reported here agree well with this hypothesis. Moreover, the added dimension provided by temperature in connection with the binding of natural and unnatural ligands of IFABP supports a view whereby equilibria between different conformational states can be poised at will. Remarkably, our data point to the existence of a different mode of interaction between IFABP and bisANS. Figure 12 shows a general model that involves the interaction of IFABP with bisANS and oleic acid. In the proposed model, IFABP has two binding sites for bisANS, one of them (I) being the fatty acid binding pocket ($bisANS_I$−IFABP) and the second (II) being a site exclusive for bisANS ($bisANS_{II}$−IFABP). The affinity of this ligand for binding site II decreases when the fatty acid is bound to the protein (i.e., the value of K_{d2} (value of K_d obtained by titration of holo-IFABP with bisANS) is significantly greater than the value of K_{d1} obtained from the corresponding titration curve of apo-IFABP). A good fit was obtained of the model proposed in Figure 12 to the experimental data from titration of IFABP with bisANS (in the presence or in the absence of oleic acid) and competition experiments at 28 and 39 °C. The values of K_d are listed in the legend to Figure 12. These simulations took into account a range of values of K_{d5} (0.1−0.8 μM) consistent with the different values for this constant reported in the literature.

In light of these results, we propose the tentative model shown in Figure 13, which includes both the thermal transition and the ligand binding equilibria. In brief, we postulate at least three different conformations for IFABP, namely, ordered (I), locally disordered (II), and altered (III). The apo-form of IFABP would coexist as two distinct thermally interconvertible states (IFABPo and IFABPd, see ref *12*). At low temperatures or in the presence of oleic acid, the ordered conformation (I) would be favored, a state homologous to that described for this and for other proteins of the same family (*6*−*8*). At variance with the behavior observed with the natural ligand, ANS does not appear to induce order in the protein, rather the ANS-bound complex structurally resembles the apo-form. The most direct evidence for this is given by the proteolytic assays, where IFABP complexed to ANS shows the same pattern as that of the apo-protein. On the other hand, a more complex behavior is observed when bisANS is bound to IFABP. In this case, bisANS is able to probe a subpopulation of IFABP, which would show a different conformation from that prevalent in the apo-protein. In this context, temperature would be the main driving force leading to this form in the conformational ensemble.

Free Energy of Conformational Transition vs Free Energy of Binding to bisANS. In the model proposed in Figure 13, a new binding site for bisANS would appear in the disordered form of IFABP (IFABPd), a species that would prevail at high temperature. With the aim of evaluating the possible influence of the binding of bisANS on the thermal equilibrium, we compared the magnitude of the free energy change associated with the thermal transition (ΔG_t) to the free energy changes associated with the binding of the ligand bisANS (ΔG_1, ΔG_2, and ΔG_3; Figure 14). From the CD data obtained in an earlier work (*12*), we estimated the value of the equilibrium constant at 39 °C, a temperature close to the midpoint of the thermal transition, according to a classical approach used to calculate ΔG in protein thermal denaturation experiments (*39*). On the other hand, we estimated the

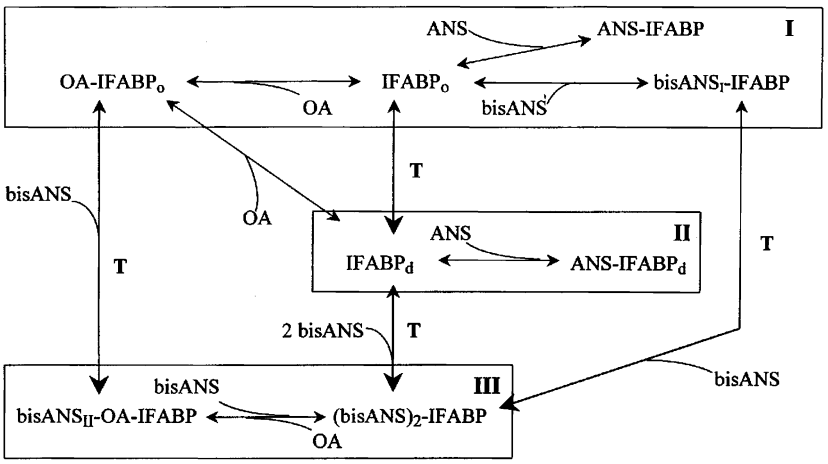

FIGURE 13: Temperature and bisANS binding reveal different conformations of IFABP. Boxes I−III indicate the three conformations of IFABP, namely, ordered (I), locally disordered (II), and altered (III), which interconvert upon changes in temperature and/or ligand binding. OA-IFABP$_o$ represents the protein bound to oleic acid; IFABP$_o$ and IFABP$_d$ denote the protein species ordered or locally disordered, respectively; and T indicates those processes favored by an increase in temperature in the direction shown by the large head arrows.

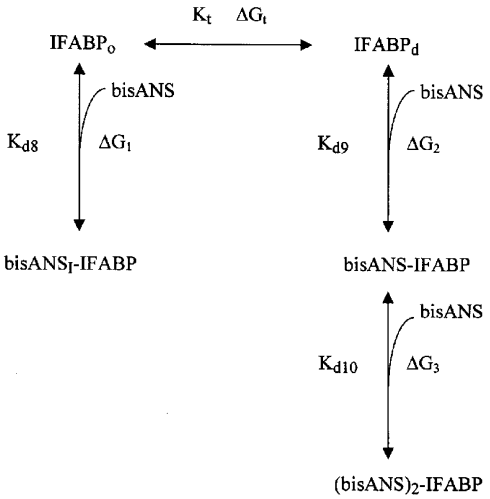

FIGURE 14: Influence of bisANS binding on the thermal transition of IFABP. K_t is the thermodynamic constant associated to the thermal transition, whereas K_{d8}−K_{d10} are the dissociation constants for the binding of bisANS to IFABP. The differences $\Delta\Delta G$ (= $\Delta G_2 + \Delta G_3 - \Delta G_1$) calculated at 39 °C for 1, 10, and 30 μM bisANS were −0.47, 0.96, and 1.65 kcal/mol. For this analysis K_{d9} and K_{d10} were estimated as $1/K_{d9} = 1/K_{d1} + 1/K_{d3}$ and $K_{d10} = K_{d4} + K_{d6}$ (see Figure 12), and K_{d8} was equated to the value of K_d at 28 °C reported in Table 1.

difference in the free energy of binding at concentrations of ligand typically used in fluorescence experiments (1, 10, and 30 μM) according to

$$\Delta G_{x\mu M} = \Delta G^\circ_{1M} + RT \ln Q,$$

$$\text{where } \Delta G^\circ_{1M} = -RT \ln K_d \text{ and } Q = \frac{[\text{free form}][L]}{[\text{bound form}]} \quad (10)$$

The thermal equilibrium will be affected by the binding equilibria inasmuch as the difference $\Delta\Delta G = \Delta G_2 + \Delta G_3 - \Delta G_1$ becomes significant with respect to ΔG_t. The comparison between these values (see legend to Figure 14) indicates that it is energetically unlikely that the binding of the ligand could bear a major influence on the conformational transition of IFABP for the range of concentrations of bisANS typically used in the present work (1−30 μM).

Alternatively, the following analysis could be undertaken to estimate the mutual influence between both associated equilibria. The apparent thermal equilibrium in the presence of bisANS may be defined as follows:

$$K_{tapp} = \frac{[P_d] + [LP_d] + [L_2P_d]}{[P_o] + [LP_o]} \quad (11)$$

where L = bisANS; P_o = IFABP$_o$; P_d = IFABP$_d$; $K_t = [P_d]/[P_o]$; $K_{d8} = [L][P_o]/[LP_o]$; $K_{d9} = [L][P_d]/[LP_d]$; and $K_{d10} = [L][LP_d]/[L_2P_d]$.

Substitution of each of the latter equations in eq 11 leads to the following expression:

$$K_{tapp} = K_t \frac{(1 + [L]/K_{d9} + [L]^2/K_{d9}K_{d10})}{(1 + [L]/K_{d8})} \quad (12)$$

Here, if L < K_{d8}, K_{d9}, K_{d10}, then $K_{tapp} \sim K_t$; if L ~K_{d8}, K_{d9}, K_{d10}, then $K_{tapp} \sim 1.5\ K_t$; and if L ~3K_{d8}, 3K_{d9}, 3K_{d10}, then $K_{tapp} \sim 3.3\ K_t$. Thus, it is expected that only a minor variation in the thermal equilibrium would occur at a typical concentration of bisANS as used in these assays.

Although we have no direct structural information on the precise location of the second binding site for bisANS, it is possible that a favorable charge interaction would take place between negatively charged bisANS and the highly positively charged region located in the helical domain of IFABP. However, electrostatics alone cannot fully explain the behavior observed (see Figure 2). Interestingly, this could be a phenomenon analogous to the interaction proposed by others (*37*, *40*) between this same domain and acidic phospholipid vesicles, which would lead to a disordered state of the protein enhancing fatty acid release. In our case, two evidences support this proposal: (i) at least one sulfonate group of bisANS lies close to residue R28 of IFABP (~6 Å) in the model proposed for the complex (*12*) and (ii) the unique pattern of proteolysis of bisANS/IFABP complexes shown in this paper indicates an enhanced cleavage at R28. In summary, our contention holds that bisANS, rather than acting in this case as an inducer molecule, reveals the altered nature of this conformational state.

Conclusion. This work highlights the importance of subtle (and reversible) changes in protein conformation, which modulate the binding activity of IFABP. With the aid of the

fluorescent probe bisANS, a different conformation of IFABP was characterized that is more populated at higher temperatures. This fact stresses the high flexibility that this protein exhibits at defined locations, while maintaining its overall conformation.

Our results point to the dynamic role played by the entry portal region of IFABP, which might possibly serve to confer the protein a physiologically important discriminating ability toward different hydrophobic ligands and which might enable it to traffic fatty acids to and from cellular membranes.

ACKNOWLEDGMENT

We thank Dr. Rolando C. Rossi for his advice on protein−ligand equilibria and Ms. Lucrecia Curto for her assistance with FPLC runs.

SUPPORTING INFORMATION AVAILABLE

Detailed spectra information about energy transfer from IFABP to ANS and bisANS, far and near UV dichroic spectra of IFABP associated to ANS and bisANS, and size-exclusion chromatography of apo-IFABP and bisANS−IFABP (Figures S1−S4). This material is available free of charge via the Internet at http://pubs.acs.org.

REFERENCES

1. Glatz, J. F., and van der Vusse, G. J. (1996) *Prog. Lipid Res. 35*, 243.
2. Jones, T. A., Bergfors, T., Sedzik, J., and Unge, T. (1988) *EMBO J. 7*, 1597.
3. Chytil, F., and Ong, D. E. (1987) *Annu. Rev. Nutr. 7*, 321.
4. Pastuszyn, A., Noland, B. J., Bazan, J. F., Fletterick, R. J., and Scallen, T. J. (1987) *J. Biol. Chem. 262*, 13219.
5. Banaszak, L., Winter, N., Xu, Z., Bernlohr, D. A., Cowan, S., and Jones, A. (1994) *Adv. Protein Chem. 45*, 89.
6. Hodsdon, M. E., Ponder, J. W., and Cistola, D. P. (1996) *J. Mol. Biol. 264*, 585.
7. Hodsdon, M. E., and Cistola, D. P. (1997) *Biochemistry 36*, 1450.
8. Hodsdon, M. E., and Cistola, D. P. (1997) *Biochemistry 36*, 2278.
9. Jamison, R. S., Newcomer, M. E., and Ong, D. E. (1994) *Biochemistry 33*, 2873.
10. LiCata, V. J., and Bernlohr, D. A. (1998) *Proteins: Struct., Funct., and Genet. 33*, 577.
11. Likić, V. A., and Prendergast, F. G. (1999) *Protein Sci. 8*, 1649.
12. Arighi, C., Rossi, J. P. F. C., and Delfino, J. M. (1998) *Biochemistry 37*, 16802.
13. Daniel, E., and Weber, G. (1966) *Biochemistry 5*, 1893.
14. Lakowicz, J. (1986) *Principles of Fluorescence Spectroscopy*, pp 43, Plenum Press, New York and London.
15. Weber, G. (1992) *Protein Interactions*, pp 177, Chapman & Hall, Inc., New York.
16. Eftink, M. (1997) *Methods Enzymol. 278*, 221.
17. Scatchard, G. (1949) *Ann. NY Acad. Sci. 51*, 660.
18. Wu, P., and Brand, L. (1994) *Anal. Biochem. 218*, 1.
19. Fairclough, R. H., and Cantor, C. R. (1978) *Methods Enzymol. 48*, 347.
20. Dalessio, P. M., and Ropson, I. J. (2000) *Biochemistry 39*, 860.
21. Clérico, E. M., Peisajovich, S. G., Ceolín, M., Ghiringhelli, P. D., and Ermácora, M. R. (1999) *Biochim. Biophys. Acta 1476*(2), 205.
22. Klimtchuk, E., Wessels, W., Kirk, W., Kurian, S., Mordi, A., and Prendergast, F. (1998) *Protein Sci. 7*, supp. 1, 450-M.
23. Schmid, F. X. (1989) in *Protein Structure: a practical approach* (Creighton T. E., Ed.) p 251, IRL, Oxford, UK.
24. Schägger, H., and von Jagow, G. (1987) *Anal. Biochem. 166*, 368.
25. Laurière, M. (1993) *Anal. Biochem. 212*, 206.
26. Kirk, W. R., Kurian, E., and Prendergast, F. G. (1996) *Biophys. J. 70*, 69.
27. Kane, C. D., and Bernlohr, D. A. (1996) *Anal. Biochem. 233*, 197.
28. Kurian, E., Kirk, W. R., and Prendergast, F. G. (1996) *Biochemistry 35*, 3865.
29. Seale, J. W., Martinez, J., and Horowitz, P. M. (1995) *Biochemistry 34*, 7443.
30. Seale, J. W., Brazil, B. T., and Horowitz, P. M. (1998) *Methods Enzymol. 290*, 318.
31. Richieri, G. V., Ogata, R. T., and Kleinfeld, A. M. (1995) *J. Biol. Chem. 270*, 15076.
32. Richieri, G. V., Ogata, R. T., and Kleinfeld, A. M. (1996) *J. Biol. Chem. 271*, 11291.
33. Alberg, D. G., and Schreiber, S. L. (1993) *Science 262*, 248.
34. Yang, D., Rosen, M. K., and Schreiber, S. L. (1993) *J. Am. Chem. Soc. 115*, 819.
35. Shi, L., Palleros, D. R., and Fink, A. L. (1994) *Biochemistry 33*, 7536.
36. Wiesner, S., Kurian, E., Prendergast, F. G., and Halle, B. (1999) *J. Mol. Biol. 286*, 233−246.
37. Corsico, B., Cistola, D. P., Frieden, C., and Storch J. (1998) *Proc. Natl. Acad. Sci. U.S.A. 95*, 12174.
38. Cistola, D. P., Kim, K., Rogl, H., and Frieden, C. (1996) *Biochemistry 35*, 7559.
39. Pace, C. N., Shirley, B. A., and Thomson, J. A. (1989) *Protein structure: a practical approach* (Creighton, T. E., Ed.) p 311, IRL, Oxford, UK.
40. Hsu, K., and Storch, J. (1996) *J. Biol. Chem. 271*, 13317.
41. Yoo, S. H., Albanesi, J. P., and Jameson, D. M. (1990) *Biochim. Biophys. Acta 1040*, 66.

BI020680D